Available online at www.sciencedirect.com
ScienceDirect
Journal of Solid State Chemistry 180 (2007) 2859–2863
JOURNAL OF SOLID STATE CHEMISTRY
www.elsevier.com/locate/jssc

Long-range magnetic ordering in Ba_2CoS_3: A neutron diffraction study

D.A. Headspith[a], P.D. Battle[b], M.G. Francesconi[a,*]

[a]*Department of Chemistry, University of Hull, Cottingham Road, Hull HU6 7RX, UK*
[b]*Inorganic Chemistry Laboratory, Oxford University, South Parks Road, Oxford OX1 3QR, UK*

Received 1 May 2007; received in revised form 19 July 2007; accepted 30 July 2007
Available online 22 August 2007

Abstract

Neutron powder diffraction has been used to determine the magnetic structure of the quasi-one-dimensional compound Ba_2CoS_3, which contains linear [001] chains of vertex-sharing CoS_4 tetrahedra, spaced apart by Ba^{2+} cations. At 1.5 K the Co^{2+} cations in the chains are antiferromagnetically ordered with an ordered magnetic moment of 1.97(4) μ_B per cation aligned along [100]. Each Co^{2+} cation is ferromagnetically aligned with four cation in neighbouring chains and antiferromagnetically aligned with two others.

Keywords: One-dimensional sulphides; Neutron diffraction; Magnetic structure

1. Introduction

Historically, research into the electronic properties of inorganic solids has focussed on oxides, mainly because the preparation and characterisation of non-oxide compounds presents more experimental challenges. Nevertheless, progress in synthetic methods has encouraged the preparation of a wider range of non-oxide materials, for example nitrides and sulphides [1]. It has become apparent that these materials can make an important contribution to the study of magnetic interactions in solids in which anions mediate magnetic coupling between transition metal cations [2]. Low-dimensional magnetic interactions take place between localised unpaired electrons along a chain of cations (one-dimensional (1-D) structures) or amongst the cations in a plane (one-dimensional (2-D) structures) and are mediated by the anions bridging the transition metals. The relatively high polarisability of the sulphide ion relative to the oxide ion ensures that sulphides are in general less ionic than oxides, and that low-dimensional structures therefore occur more frequently in sulphides. The preparation and characterisation of new inorganic sulphides can thus make a significant contribution to the development of our understanding of low-dimensional magnetism. The characterisation of 1-D materials is particularly welcome, as these systems are rarer than 2-D materials [3]. We describe below the determination by neutron diffraction of the magnetic structure of one such compound, Ba_2CoS_3, in which corner-linked CoS_4 tetrahedra form 1-D chains [4]. We have previously shown that this phase exhibits metallic-like behaviour and negative magnetoresistance, making it the first 1-D sulphide containing Co^{2+} to do so [5].

The synthesis and antiferromagnetic properties of Ba_2CoS_3 were originally reported by Nakayama et al. [6] but no structural details were given. In 1972, Hong and Steinfink [7] reported the crystal structures of a number of phases within the Ba–Fe–S(Se) system, among them Ba_2FeS_3 which is isostructural with Ba_2CoS_3, but again no detailed crystallographic data were given. Our own previous structural study, based on the Rietveld analysis of X-ray diffraction data collected from a polycrystalline sample of Ba_2CoS_3, showed that the unit cell is orthorhombic with parameters $a = 12.000(1)$ Å, $b = 12.470(1)$ Å and $c = 4.205(2)$ Å [8]. Ba^{2+} occupies two distinct crystallographic sites, both coordinated by S^{2-} in a prismatic fashion. One Ba^{2+} is surrounded by six S^{2-} ions at the corners of a trigonal prism and an additional S^{2-} is approximately centred above one rectangular face. Seven S^{2-} ions also surround the other Ba^{2+} forming a distorted trigonal prism with one face capped. The CoS_4 tetrahedra,

*Corresponding author. Fax: +44 1482 46 6410.
E-mail address: m.g.francesconi@hull.ac.uk (M.G. Francesconi).

0022-4596/$ - see front matter © 2007 Elsevier Inc. All rights reserved.
doi:10.1016/j.jssc.2007.07.029

which form chains along the z direction, are heavily distorted, with the two Co–S bridging bonds stretched along the chain direction. Those bond lengths are 2.427(2) Å, which is significantly longer than the two terminal Co–S bonds, 2.330(3) and 2.317(3) Å. The S–Co–S bond angles deviate from 109.5° by up to several degrees. The tetrahedra are not only elongated along the crystallographic z direction, which would yield a C_{2v} local point group, but further distorted to a C_s subgroup [8]. The distortion of the local structure of Co^{2+} was confirmed by investigations performed on Ba_2CoS_3 by EXAFS and XANES [8]. The distance between Co^{2+} cations within each chain (intra-chain) is 4.205(1) Å, whereas the distances between Co^{2+} cations in two neighbouring chains (inter-chain) are 6.153(3) and 6.582(3) Å. Neighbouring chains of Co–S tetrahedra are separated by Ba–S blocks, thus conferring 1-D character on the structure, which is drawn in Fig. 1.

We supported our experimental work with ab-initio calculations, which suggested that the Co^{2+} cations are in a high-spin state ($S = 3/2$). Using a perturbative approach, we predicted the intra-chain coupling between nearest-neighbour Co^{2+} cations via a Co–S–Co super exchange pathway to be antiferromagnetic [8]. This is consistent with the temperature dependence of the magnetic susceptibility, which showed a broad maximum at ~135 K, indicative of 1-D antiferromagnetic coupling between the Co^{2+} cations [6]. The inverse susceptibility was not a linear function of temperature below 380 K, and therefore could not be modelled using the Curie–Weiss Law. More sophisticated analyses of the high-temperature susceptibility indicated that Ba_2CoS_3 can be considered to be a Heisenberg system, in agreement with literature reports that Co^{2+} in such a distorted tetrahedral environment generally exhibits almost isotropic g values in the range 2.2–2.4 [9,10]. Our subsequent analyses showed that susceptibility was best described over a wide temperature range using a 1-D Wagner–Friedel model [9] with an intra-chain exchange constant $J = -37 \pm 2$ K and a Landé factor $g = 2.36 \pm 0.01$. However, no real compound is truly 1-D and, although the estimated value of the antiferromagnetic inter-chain coupling constant ($J'' \approx -1$ K) certainly permits the description of Ba_2CoS_3 as a quasi-1-D system, the temperature dependence of both the susceptibility and the heat capacity data showed evidence, albeit only a subtle change in gradient, for the onset of 3-D long-range antiferromagnetic ordering in Ba_2CoS_3 at 46 K [5,8]. We have now proved the existence of an antiferromagnetic ground state by neutron diffraction and the details of the magnetic structure adopted are described below.

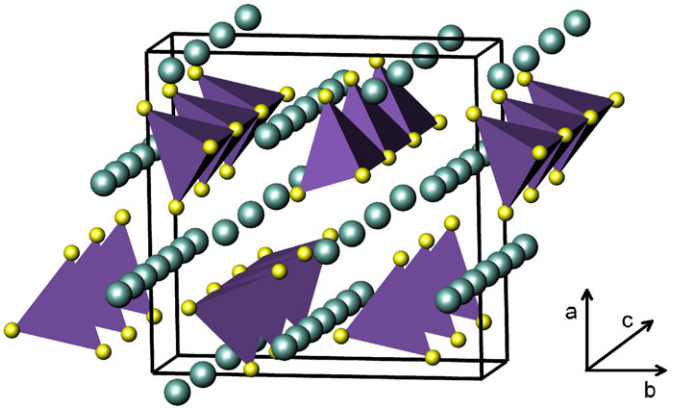

Fig. 1. (Color online.) The Ba_2CoS_3 structure showing the chains of CoS_4 corner-linked tetrahedra along the c-axis: the large and small (green and yellow) spheres represent the Ba^{2+} and S^{2-} ions, respectively.

2. Experimental

The synthesis of a 4 g polycrystalline sample of Ba_2CoS_3 was achieved via a solid–gas reaction between CS_2 and a stoichiometric mixture of powdered $BaCO_3$ and $CoCO_3$. Carbon disulphide is a liquid with a low vapour pressure. If nitrogen gas is bubbled through liquid CS_2, the gas acts as a carrier and a vapour of N_2/CS_2 can be passed through a tubular furnace. The nitrogen gas was first passed through concentrated sulphuric acid in order to remove any moisture and then through a Dreschel bottle containing liquid CS_2, which was in turn connected to the silica work tube of the furnace. Nitrogen gas was used to flush the system of air before the reaction was started, and to remove CS_2 once the reaction was completed. The downstream end of the silica tube was connected to another Dreschel bottle containing paraffin oil, which sealed the system from the air and acted as a post-reaction scrubber, thus reducing the release of any residual CS_2.

The ground mixture of $BaCO_3$ and $CoCO_3$ was contained in a carbon boat and heated at 1000 °C under a flow of CS_2/N_2 for 48 h with intermittent re-grinding. At the end of the reaction, the product was cooled slowly to room temperature.

High-resolution neutron powder diffraction data were collected on the D2b diffractometer at the Institut Laue-Langevin (ILL), Grenoble, using a wavelength $\lambda = 2.3975$ Å and covering the angular range $10 \leqslant 2\theta/^\circ \leqslant 140$ with a step size $\Delta 2\theta = 0.05^\circ$. The sample was contained in a vanadium can of internal diameter 8 mm. Data were collected for 8 h at both 200 and 1.5 K; the relatively long collection times were a consequence of the weakness of the observed scattering. The powder diffraction data were analysed by profile analysis [11] as implemented in the GSAS suite of programs [12,13]. The background was described by a 12-term Chebyschev polynomial and the peak shape by a multi-term Simpson's rule integration of the pseudo-Voigt function described by Howard [14]. No absorption correction was applied.

3. Results

Neutron diffraction data were collected at 200 K, well above both the susceptibility maximum and the specific heat anomaly, to ensure that the data contained no magnetic Bragg scattering. These data could be analysed

using the structure determined previously by X-ray diffraction at room temperature as a starting model. It was, however, necessary to use a two-phase refinement in order to account for a crystalline BaS [15] impurity which was always present in the reaction product. No corresponding crystalline Co-containing impurity could be identified, although the use of a stoichiometric mixture of reactants requires that one must be present. Despite the use of an extended data-collection time, the signal-to-noise ratio was relatively poor. However, the Bragg peaks were not unusually broad, and the crystallinity of the Ba_2CoS_3 phase in our sample is therefore not in doubt. The presence of an amorphous or poorly-crystalline Co-containing impurity phase might be responsible for the high background level observed. The refinement involved the unit cell parameters for the two phases, the counter zero point, 1 scale factor, 2 phase fractions, 12 atomic coordinates, 6 isotropic atomic displacement parameters, 6 profile parameters and 12 background parameters. The displacement parameters of all atoms of a particular element were constrained to be equal. Quantitative determination of BaS showed that the sample contained, by weight, 11.4(6)% of this secondary phase. The residual fit parameters are $R_{wp} = 0.0514$, $R_p = 0.0403$, DW-d = 0.517 and $\chi^2_{red} = 5.068$. The observed and calculated diffraction profiles are shown in Fig. 2, the structural parameters are listed in Table 1 and the interatomic distances in Table 2. The broad peak in the difference profile at $2\theta \sim 45^\circ$ might be attributable to the Co-containing impurity discussed above. The poor fit to the profile below $2\theta \sim 40^\circ$ is attributable to the presence of modulations in the diffuse background scattering that are not be modelled by our analysis. We shall return to this point below. The fit to the data at high angles is clearly better than that at low angles.

Comparison of the neutron data sets collected at 200 K and at 1.5 K revealed a number of extra sharp peaks in the low-angle region of the latter. These peaks could not be accounted for using the orthorhombic unit cell of Ba_2CoS_3 and were therefore assumed to be attributable to magnetic Bragg scattering associated with the onset of long-range antiferromagnetic order.

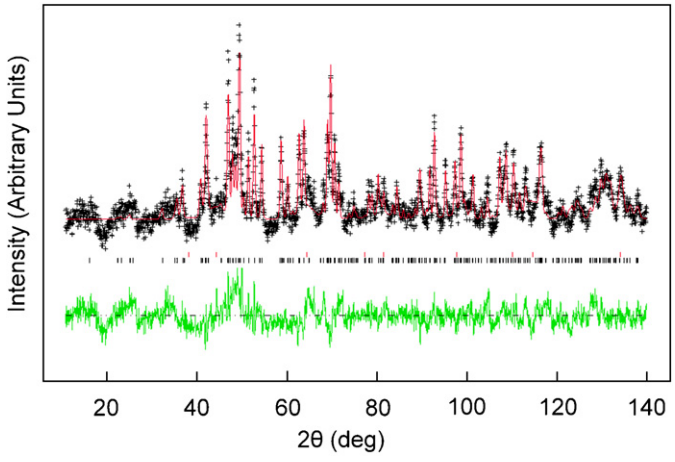

Fig. 2. (Color online.) Neutron diffraction profiles for Ba_2CoS_3 at 200 K, showing background-subtracted observed (+), calculated (red line) and difference (green line) patterns. Tick marks indicate reflection positions for the BaS (upper) and Ba_2CoS_3 (lower) phases.

Table 1
Structural parameters for Ba_2CoS_3 derived from neutron data collected at 200 K

Atom	Site	x	y	z	U_{iso} (Å^2)
Ba(1)	4c	0.3254(8)	0.0177(8)	$\frac{1}{4}$	0.026(3)
Ba(2)	4c	0.9842(8)	0.8245(8)	$\frac{1}{4}$	0.026(3)
Co	4c	0.251(2)	0.310(2)	$\frac{1}{4}$	0.033(8)
S(1)	4c	0.3638(13)	0.4458(12)	$\frac{1}{4}$	0.021(4)
S(2)	4c	0.0616(13)	0.3590(14)	$\frac{1}{4}$	0.021(4)
S(3)	4c	0.7206(13)	0.7892(13)	$\frac{1}{4}$	0.021(4)

Space group *Pnam*: $a = 11.994(2)$ Å, $b = 12.472(2)$ Å, $c = 4.201(1)$ Å, $V = 628.5(3)$ Å^3.

Table 2
Selected bond lengths and angles in Ba_2CoS_3 from neutron data collected at 200 K

Distances (Å)			
Ba(1)–Co	3.46(2) × 2	Co–S(1)	2.16(2)
	3.75(3)		
Ba(1)–S(1)	3.22(1) × 2	Co–S(2)	2.36(3)
Ba(1)–S(2)	3.19(2) × 2	Co–S(3)	2.46(1) × 2
	3.22(2)		
Ba(1)–S(3)	3.24(2) × 2		
Ba(2)–Co	3.81(2) × 2		
Ba(2)–S(1)	3.17(1) × 2	Co–Co (intrachain)	4.2010(7)
	3.21(2)		
Ba(2)–S(2)	3.16(2) × 2		6.182(10),
Ba(2)–S(3)	3.19(2)	(interchain)	6.5807(10)
	3.17(2)		
Angles (deg)			
S(1)–Co–S(2)	113.6(11)	S(2)–Co–S(3)	105.2(6)
S(1)–Co–S(3)	108.0(7)	S(3)–Co–S(3)	117.1(10)

The data were fitted via a three-phase refinement, using the structural parameters calculated from the 200 K data as models for the crystallographic unit cells of Ba_2CoS_3 and BaS. The simplest unit cell that could account for all the reflections associated with the magnetic ordering was orthorhombic with $a_{mag} = a_{cryst}$, $b_{mag} = b_{cryst}$ and $c_{mag} = 2c_{cryst}$. The magnetic unit cell thus contained eight Co cations. A model for the spin-ordering pattern was devised by assuming that neighbouring spins in each [001] chain couple antiferromagnetically, and then identifying the inter-chain spin arrangement that best fitted the data. The Miller indices of the strong magnetic reflections (001 and 110) ruled out all B-centred structures. Good agreement was achieved with the magnetic structure shown in Fig. 3 and described in Table 3; following a number of trial refinements, the atomic magnetic moments, assumed to be equal for all Co atoms, were constrained to lie along [100]. The ordered magnetic moment refined to a value of

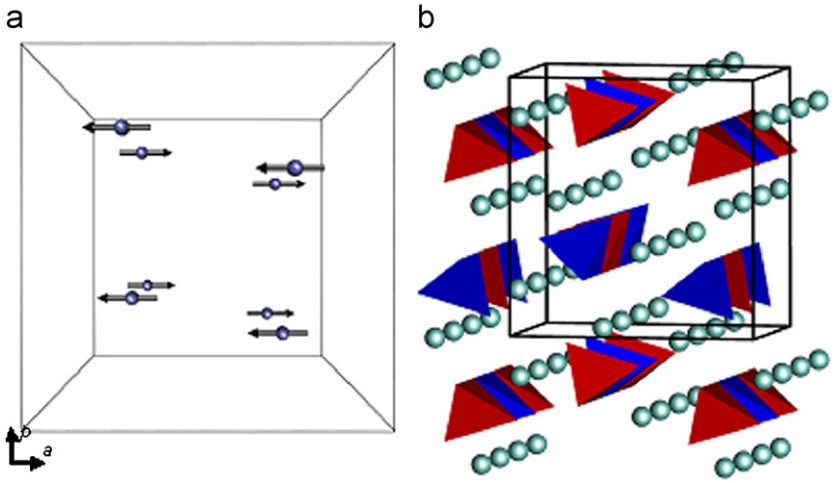

Fig. 3. (a) View of the Ba_2CoS_3 magnetic unit cell along [001] showing the alignment of the spin vectors on the Co^{2+} cations and (b) perspective view showing the CoS_4 tetrahedra and the Ba cations (grey spheres; green online); the different colours of the tetrahedra highlight the different spin directions of the Co^{2+} cations.

Table 3
Structural parameters for the magnetic unit cell of Ba_2CoS_3 at 1.5 K

Atom	x	y	z	m_x (μ_B)
Co(1)	0.246(1)	0.307(1)	0.1250	+1.97(4)
Co(2)	0.254(1)	0.807(1)	0.3750	+1.97(4)
Co(3)	−0.246(1)	−0.307(1)	0.3750	+1.97(4)
Co(4)	0.746(1)	0.193(1)	0.1250	+1.97(4)
Co(5)	0.246(1)	0.307(1)	0.6250	−1.97(4)
Co(6)	0.246(1)	0.807(1)	0.8750	−1.97(4)
Co(7)	−0.246(1)	−0.307(1)	0.8750	−1.97(4)
Co(8)	0.786(1)	0.193(1)	0.6250	−1.97(4)

$a_{mag} = 11.971(1)$ Å, $b_{mag} = 12.443(1)$ Å, $c_{mag} = 8.3781(8)$ Å, $V = 1248.0(3)$ Å^3.

Table 4
Structural parameters for the crystallographic unit cell of Ba_2CoS_3 at 1.5 K

Atom	Site	x	y	z	U_{iso}
Ba(1)	4c	0.3269(5)	0.0187(5)	$\frac{1}{4}$	0.011(2)
Ba(2)	4c	0.9866(5)	0.8266(5)	$\frac{1}{4}$	0.011(2)
Co	4c	0.2463(12)	0.3071(11)	$\frac{1}{4}$	0.025(5)
S(1)	4c	0.3648(9)	0.4443(8)	$\frac{1}{4}$	0.016(2)
S(2)	4c	0.0612(9)	0.3622(9)	$\frac{1}{4}$	0.016(2)
S(3)	4c	0.7259(8)	0.7915(9)	$\frac{1}{4}$	0.016(2)

Space group *Pnam*: $a_{cryst} = 11.971(1)$ Å, $b_{cryst} = 12.443(1)$ Å, $c_{cryst} = 4.1890(4)$ Å, $V = 624.0(2)$ Å^3.

1.97(4) μ_B per Co^{2+}. This model cannot be distinguished from one in which the relative phase of spins in chains with a relative displacement of $c_{mag}/4$ is reversed, that is one in which the moments of Co2, Co6, Co3 and Co7 are all reversed. No other model was found that gave a comparable level of agreement. The phase fraction of BaS refined to a value of 10.3(2)%, which is not significantly different

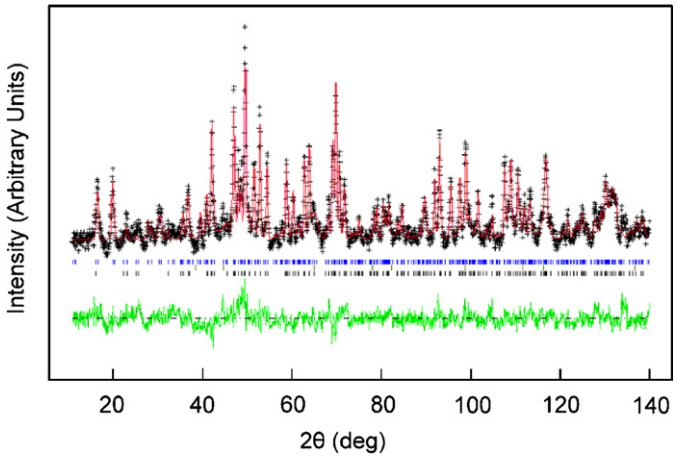

Fig. 4. (Color online.) Neutron diffraction profiles for Ba_2CoS_3 at 1.5 K, showing background-subtracted observed (+), calculated (red line) and difference (green line) patterns. Tick marks indicate reflection positions for the magnetic unit cell (upper), BaS (middle) and structural unit cell (lower).

from the value derived in the analysis of the data collected at 200 K. The refined structural parameters are presented in Table 4. The residual fit parameters were $R_{wp} = 0.0467$, $R_p = 0.0364$, DW-d = 0.612 and $\chi^2_{red} = 4.931$. The resulting profile fit is shown in Fig. 4. The most obvious feature in the difference profile is that at $2\theta \sim 45^\circ$, as it was for the data set collected at 200 K. It therefore cannot be magnetic in origin. The quality of the fit varies less with angle than was the case for the data collected at 200 K.

4. Discussion

As we discussed above, the synthetic methods that must be used in order to prepare sulphides often produce multiphasic reaction products, and that is certainly true in the case of Ba_2CoS_3. However, although our sample is imperfect, we have been able to refine the crystal structure

of Ba_2CoS_3 at 200 K and the magnetic structure at 1.5 K. The structural parameters obtained from the analysis of the neutron diffraction data collected at 200 K are in good agreement with those previously obtained from X-ray diffraction data collected at room temperature. In particular, the Co–S bond lengths and angles confirm that Co^{2+} is in a highly distorted tetrahedral environment. However, the agreement between the observed and calculated diffraction profiles is poor in the region $2\theta < 40^\circ$, where we have not modelled the broad features visible in the diffuse scattering. The level of agreement in this region is much better for the data set collected at 1.5 K. We therefore tentatively ascribe the features observed at 200 K to magnetic diffuse scattering caused by the onset of 1-D magnetic order, with magnetic Bragg peaks developing in this angular region on cooling below the Néel temperature. This interpretation is consistent with the susceptibility and heat capacity data which suggest that 1-D ordering is developing at 200 K, and that long-range ordering is observed below $T_N = 46$ K. However, we must emphasise the speculative nature of this hypothesis. The existence of an antiferromagnetic ground state is proved by our neutron diffraction study. The magnetic structure drawn in Fig. 3 involves antiferromagnetic coupling along the [001] chains of CoS_4 tetrahedra. Each Co^{2+} cation has two nearest neighbours to which it is antiferromagnetically coupled, and the six next-nearest Co^{2+} neighbours are more than 6 Å distant. Ferromagnetic alignment occurs with four of these next-nearest neighbours, and antiferromagnetic with the remaining two, thus emphasising the dominance of the nearest-neighbour interactions. However, the relatively high Néel temperature of Ba_2CoS_3 shows that the next-nearest-neighbour interactions are too strong for this compound to be regarded as a model 1-D magnetic system, despite the presence of isolated chains of transition metal polyhedra in the crystal structure. The ordered magnetic moment of the Co^{2+} cations is significantly lower than the spin-only value ($3\,\mu_B$). This suggests that the distortion of the tetrahedral site is sufficient to quench any orbital contribution to the ordered moment, and that the value is further reduced as a consequence of covalency in the Co–S bonds. By way of comparison, the ordered moment in the spinel Co_3O_4, in which Co^{2+}–O bonds form a regular tetrahedron has been reported to be $2.70(1)\,\mu_B$ per Co^{2+} cation [16].

In conclusion, we have proved that Ba_2CoS_3 shows 3-D antiferromagnetic ordering at 1.5 K, thus removing the uncertainty associated with earlier interpretations of susceptibility and heat capacity data. The previously identified [8] strong superexchange interaction between Co^{2+} cations in the chains of vertex-linked CoS_4 tetrahedra that lie parallel to [001] dictates the long-range-ordered magnetic structure adopted.

Acknowledgments

We are grateful to the EPSRC for funding the recent upgrade of the D2b diffractometer (GR/R88601), and to A.W. Hewat for his assistance at ILL.

References

[1] P. Vaqueiro, A.V. Powell, Chem. Mater. 12 (9) (2000) 2705–2714.
[2] W. Bronger, P. Müller, J. Alloy Compd. 246 (1997) 27–36.
[3] L.J. De Jongh, A.R. Miedema, Adv. Phys. 23 (1974) 1–260.
[4] T. Baikie, A. Maignan, M.G. Francesconi, Chem. Commun. 7 (2004) 836–837.
[5] T. Baikie, V. Hardy, A. Maignan, M.G. Francesconi, Chem. Commun. 40 (2005) 5077–5079.
[6] N. Nakayama, K. Kosuge, S. Kachi, T. Shinjo, T. Takada, J. Solid State Chem. 33 (1980) 351–356.
[7] H.Y. Hong, H. Steinfink, J. Solid State Chem. 5 (1972) 93–98.
[8] A.J.D. Barnes, T. Baikie, V. Hardy, M.B. Lepetit, A. Maignan, N.A. Young, M.G. Francesconi, J. Mater. Chem. 16 (2006) 3489–3502.
[9] V.M. García, O. Castell, R. Caballol, J.P. Malrieu, Chem. Phys. Lett. 238 (1995) 222–229;
V.M. García, M. Reguero, R. Caballol, Theor. Chem. Acc. 98 (1997) 50–56.
[10] A.V. Palii, B.S. Tsukerblat, E. Coronado, J.M. Clemente-Juan, J.J. Borrás-Almenar, Inorg. Chem. 42 (7) (2003) 2455–2458.
[11] H.M. Rietveld, J. Appl. Crystallogr. 2 (1969) 65–71.
[12] B.H. Toby, J. Appl. Crystallogr. 34 (2001) 210–213.
[13] A.C. Larson, R.B. Von Dreele, General structure analysis system (GSAS), Los Alamos National Laboratory Report LAUR, 2004, pp. 86–784.
[14] C.J. Howard, J. Appl. Crystallogr. 15 (1982) 615–620.
[15] H.D. Rad, R. Hoppe, Z. Anorg. Allg. Chem. 483 (1981) 7–17.
[16] C.E. Infante, D.Phil. Thesis, Oxford, 1975.